Intratumoral Delivery of IL-21 Overcomes Anti-Her2/Neu Resistance through Shifting Tumor-Associated Macrophages from M2 to M1 Phenotype

Meng Xu,*,†,[1] Mingyue Liu,*,†,[1] Xuexiang Du,*,† Sirui Li,*,† Hang Li,* Xiaozhu Li,* Ying Li,* Yang Wang,‡ Zhihai Qin,* Yang-Xin Fu,*,‡ and Shengdian Wang*

Tumor resistance is a major hurdle to anti-Her2/neu Ab–based cancer therapy. Current strategies to overcome tumor resistance focus on tumor cell–intrinsic resistance. However, the extrinsic mechanisms, especially the tumor microenvironment, also play important roles in modulating the therapeutic response and resistance of the Ab. In this study, we demonstrate that tumor progression is highly associated with TAMs with immune-suppressive M2 phenotypes, and deletion of TAMs markedly enhanced the therapeutic effects of anti-Her2/neu Ab in a HER2/neu-dependent breast cancer cell TUBO model. Tumor local delivery of IL-21 can skew TAM polarization away from the M2 phenotype to a tumor-inhibiting M1 phenotype, which rapidly stimulates T cell responses against tumor and dramatically promotes the therapeutic effect of anti-Her2 Ab. Skewing of TAM polarization by IL-21 relies substantially on direct action of IL-21 on TAMs rather than stimulation of T and NK cells. Thus, our findings identify the abundant TAMs as a major extrinsic barrier for anti-Her2/neu Ab therapy and present a novel approach to combat this extrinsic resistance by tumor local delivery of IL-21 to skew TAM polarization. This study offers a therapeutic strategy to modulate the tumor microenvironment to overcome tumor-extrinsic resistance. *The Journal of Immunology*, **2015, 194: 4997–5006.**

Targeted therapy, acting by blocking oncogenic pathways that are crucial for tumor growth and maintenance, can arrest tumor progression and induce a striking regression in molecularly defined subsets of patients. Trastuzumab, a humanized mAb to Her2/neu, improves overall survival when given in combination with chemotherapy for metastatic disease and reduces the risk for disease recurrence and death when given in the adjuvant setting, making the drug the foundation of systemic therapy for Her2/neu-overexpressing tumors (1–3). However, a significant number of patients fail to respond to initial trastuzumab treatment, and many trastuzumab-responsive tumors develop refractory disease within 1 y of treatment (4–6). Given the increased recognition of de novo and acquired resistance to therapy, considerable research has been dedicated to understanding the molecular mechanisms of trastuzumab resistance. Although the investigations focused on tumor cells' intrinsic signaling alterations, and multiple trastuzumab-resistance mechanisms have been identified in preclinical studies, including activation of the downstream PI3K signaling pathway (7), accumulation of a constitutively active form of Her2/neu (8, 9), and cross-talk of Her2/neu with other growth factor receptors (10, 11), recent findings uncovered novel roles for the tumor microenvironment (extrinsic mechanism) in modulating therapeutic response and resistance.

In addition to blocking oncogenic signaling and inducing FcR-mediated cytotoxicity (12), recent studies by us (13, 14) and other investigators (15) showed that anti-Her2/neu Ab-mediated tumor regression also depends on adaptive immunity extrinsic to the tumor cell. Data based on immune signatures of clinical samples established that a strong immune cell component is predictive of a good response to chemotherapy, and a high T lymphocyte infiltration is associated with a higher response rate to neoadjuvant therapy in breast cancer (16). In contrast, more established tumor was shown to be more immunosuppressive, contributing to further impairment of the antitumor T cell response and tumor progression. There is growing knowledge that the tumor microenvironment contributes to chemotherapy resistance. Gene-expression analyses suggested that tumor stroma gene signature could be predictive for the resistance to neoadjuvant chemotherapy (17). Tumor-associated macrophages (TAMs) are an important component of the tumor stroma. Experimental and epidemiological studies indicate that TAMs contribute to chemoresistance and radioprotective effects. Clinical evidence showed that an elevated number of TAMs and their distinct profile correlated with therapy failure and poor prognosis in cancer patients (18, 19). A recent study showed that breast tumors with high TAM numbers and low numbers of cytotoxic T cells responded relatively poorly to chemotherapy given before surgery; blockade of macrophage recruitment into tumor, in combination with paclitaxel, improved survival of mammary tumor-bearing mice by $CD8^+$ T cell–dependent mechanisms (20).

*CAS Key Laboratory of Infection and Immunity, Institute of Biophysics, Chinese Academy of Sciences, Beijing 100101, China; †University of the Chinese Academy of Sciences, Chinese Academy of Sciences, Beijing 100049, China; and ‡Department of Pathology and Committee on Immunology, University of Chicago, Chicago, IL 60637

[1]M.X. and M.L. contributed equally to this work.

Received for publication October 15, 2014. Accepted for publication February 23, 2015.

This work was supported by the National Key Basic Research Program of China (2012CB917101 to S.W.), Natural Science Foundation of China (91231204 and 91029719 to S.W. and 31300728 to Y.L.), and National Institutes of Health Grant R01CA134563 (to Y.-X.F.)

Address correspondence and reprint requests to Dr. Shengdian Wang or Dr. Yang-Xin Fu, CAS Key Laboratory of Infection and Immunity, Institute of Biophysics, Chinese Academy of Sciences, No. 15 Datun Road, Chaoyang District, Beijing 100101, China (S.W.) or Department of Pathology and Committee on Immunology, University of Chicago, Chicago, IL 60637 (Y.-X.F.). E-mail addresses: sdwang@moon.ibp.ac.cn (S.W.) or yfu@uchicago.edu (Y.-X.F.)

The online version of this article contains supplemental material.

Abbreviations used in this article: CEL, clodronate liposome; G-MDSC, granulocytic myeloid-derived suppressor cell; i.t., intratumoral(ly); M-MDSC, monocytic myeloid-derived suppressor cell; PD-1, programmed cell death protein 1; qPCR, quantitative real-time PCR; TAM, tumor-associated macrophage; TIL, tumor-infiltrating lymphocyte.

www.jimmunol.org/cgi/doi/10.4049/jimmunol.1402603

Macrophages are highly plastic and can rapidly change their phenotypes in response to their local signals. Exposure to bacterial products and Th1 cytokines (e.g., LPS and IFN-γ) drives macrophages toward a classic (M1) activation state characterized by pro-inflammatory activity, tumoricidal function, and the promotion of T cell responses (21, 22). In response to Th2 cytokines IL-4 and IL-13, macrophages undergo alternative (M2) activation, with the ability to support tumor growth, inhibit antitumor immunity, and promote tissue repair. In malignant tumors (21, 23), TAMs resemble M2-type macrophages and are considered a promising target for tumor therapy (24). Studies of TAM-targeted therapies are primarily done by inhibiting macrophage recruitment, survival, and tumor-promoting activity in tumor, but the most potent antitumor strategy should be skewing tumor-promoting M2 TAMs to tumor-suppressive M1-type macrophages (25, 26).

In this study, we identify the abundant M2 TAMs in Her2/neu$^+$ breast tumor as a barrier to anti-Her2/neu Ab therapy. Tumor local delivery of IL-21 can skew TAM polarization from the M2 to the M1 phenotype, which reverses immunosuppression and invokes the active antitumor potential that bridges innate and T cell responses for tumor regression. Therefore, our study points to a new strategy to treat established tumor with abundant and unmanageable suppressive macrophages.

Materials and Methods

Mice

BALB/c and C57BL/6 female mice (6–8 wk) were purchased from Vitalriver Experimental Animal (Beijing, China). BALB/c Rag-1 and FVB/N-transgenic (MMTV-neu) mice were purchased from The Jackson Laboratory. All mice were maintained under specific pathogen–free conditions at the Institute of Biophysics. The study was approved by the Institutional Animal Care and Use Committee of the Institute of Biophysics, and all experiments conformed to the relevant regulatory standards.

Cell lines and reagents

TUBO, cloned from a spontaneous mammary tumor in a BALB/c Neu-transgenic mouse (27), was a gift from Joseph Lustgarten (Mayo Clinic, Scottsdale, AZ). It was cultured in 5% CO_2 and maintained in DMEM supplemented with 10% heat-inactivated FBS (HyClone), 2 mmol/l L-glutamine, 0.1 mmol/l MEM nonessential amino acids, 100 U/ml penicillin, and 100 μg/ml streptomycin.

3T3/Kb and 3T3/NKb cells were provided by Dr. Wei-Zen Wei (Wayne State University, Detroit, MI) (28). 3T3/Kb cells expressing the MHC-I molecule H2-K^d and B7.1 were maintained in supplemented DMEM (as above) with the addition of 600 μg/ml G418 and 600 μg/ml Zeocin (both from Invitrogen). 3T3/NKb cells expressing H2-K^d, B7.1, and neu Ag were maintained in supplemented DMEM with 7.5 μg/ml puromycin (Invitrogen) and 600 μg/ml G418.

Anti-neu Ab 7.16.4, produced in-house (ATCC HB-10493), recognizes the juxtamembranal region of rat neu and competes with 4D5, the precursor of trastuzumab, for binding and inhibition of tumor growth (29). Recombinant murine IL-21 (endotoxin level $<$ 1 EU/μg) was purchased from PeproTech (Rocky Hill, NJ). Murine IL-21/hFc was expressed by transient transfection of the 293E cell line with the corresponding expression plasmid and purified by protein G column (GE). Endotoxin was measured by the limulus amebocyte lysate assay (Cambrex, Walkersville, MD). For all Abs and fusion protein preparations, the amount of endotoxin was determined to be $<$0.2 EU/mg mAb (limit of detection).

In vivo treatments

TUBO cells (6–10 $\times$ 10^5) were injected s.c. in the back of 6–8-wk-old mice. Tumor volumes were measured along three orthogonal axes (a, b, and c) and calculated as tumor volume = abc/2. For combination therapy of anti-Her2/neu Ab and IL-21, 100–200 μg anti-Her2/neu Ab was injected i.p. and 5 μg IL-21 was injected intratumorally (i.t.) at the indicated time points.

Macrophage depletion was achieved by i.p. (12.5 μg) or i.t. (6.25 μg) injection of liposome suspension at the indicated time points by repeated injections every 3 or 4 d. Liposomes composed of phosphatidylcholine and cholesterol, with added dichloromethylene diphosphonate (clodronate; courtesy of Roche Diagnostics), were produced as described (30). The efficiency of macrophage depletion was assessed by CD11b and F4/80 staining.

NK cells were depleted by i.p. injection of 50 μg anti-asialo GM1 (Wako Pure Chemical Industries) 5 d before IL-21 treatment. Cell-depletion efficacy was monitored by staining peripheral blood and tumor mass for DX5.

Flow cytometry analysis and sorting

Tumor tissues were minced and digested in DMEM with 0.1% collagenase type I for 15 min at 37°C, washed, and passed through a 40-μm cell strainer. After centrifuging, cells were blocked with anti-FcR (5 μg/ml) for 10 min and incubated with the indicated Abs for 30 min at 4°C. For flow cytometry analysis, cells were acquired on a FACSCalibur (BD Biosciences), and data were analyzed with FlowJo software. For cell sorting, a FACSAria II (BD Biosciences) was used. TAMs were sorted as CD45$^+$ CD11b$^+$Gr1$^-$Ly6C$^-$F4/80$^+$CD11c$^+$ cells. Spleen was digested and stained with CD11b and F4/80 Abs. CD11b$^+$F4/80$^+$ spleen macrophages were sorted as a control for TAMs. Granulocytic myeloid-derived suppressor cells (G-MDSCs) and monocytic myeloid-derived suppressor cells (M-MDSCs) were gated as CD45$^+$CD11b$^+$Gr1$^+$Ly6C$^-$ and CD45$^+$CD11b$^+$ Gr1^{low}Ly6C$^+$, respectively.

Immunohistochemistry

Immunohistochemistry was performed on frozen sections (7 μm) of treated tumors using mAb against CD8 (clone 53-6.7), F4/80 (clone BM8), CD86 (clone P03.1), and MHC class II (clone M5/114.15.2; all from eBioscience). Briefly, sections were incubated with primary mAb (1/200) at 4°C overnight. After washing, sections were incubated with secondary Ab (anti–rat-HRP) for 30 min and positive signals were detected using DAB (both from ZSGB-BIO). Three microscope fields for each sample (n = 6) were selected, and integral OD of positive cells was assessed using Image-Pro Plus 6.0 software.

Gene-expression analysis

All mRNA analyses were performed using quantitative real-time PCR (qPCR). Briefly, total RNA of cultured cells or sorted cells was extracted by an RNeasy Kit (QIAGEN), following the manufacturer's instructions. First-strand cDNA was synthesized (NEB) and subjected to qPCR (Bio-Rad CFX96) with SYBR Green qPCR SuperMix (TransGen) using the corresponding primers. Gene expression was normalized to *β-actin* or *18s* RNA using the ΔΔCt method.

Primers

The following primers were used: *18s*: 5′-CGTCTGCCCTATCAACTTTCG-3′ and 5′-TGCCTTCCTTGGATGTGGTA-3′; *β-actin*: 5′-GCACCACACCTTCTACAA-3′ and 5′-TACGACCAGAGGCATACA-3′; *Arg2*: 5′-CACCTCTCACCACTGTATCTGG-3′ and 5′-CCAGGAAAATCCTGGCAGTTGTG-3′; *Ccl17*: 5′-GTGCTGCCTGGATTACTTCAA-3′ and 5′-GGACAGTCAGAAACACGATGG-3′; *Cxcl9*: 5′-TGCTACACTGAAGAACGGAGAT-3′ and 5′-TCCTTGAACGACGACGACTT-3′; *Il10*: 5′−7GCCAAGCCTTATCGGAAATGA-3′ and 5′-ATCACTCTTCACCTGCTCCA-3′; *Il-12p35*: 5′-ACGCAGCACTTCAGAATCAC-3′ and 5′-CGCAGAGTCTCGCCATTATG-3′; *iNos*: 5′-ACTACTGCTGGTGGTGACAA-3′ and 5′-GAAGGTGTGGTTGAGTTCTCTAAG-3′; *Mrc1*: 5′-GTTCACCTGGAGTGATGGTTCTC-3′ and 5′-AGGACATGCCAGGGTCACCTTT-3′; *Tgf-β*: 5′-CAACAATTCCTGGCGTTACCT-3′ and 5′-TGTATTCCGTCTCCTTGGTTCA-3′; *Tnf-α*: 5′-ACGCTCTTCTGTCTACTGAACT-3′ and 5′-ATCTGAGTGTGAGGGTCTGG-3′; and *Vegf*: 5′-ACGACAGAAGGAGAGCAGAA-3′ and 5′-CACAGGACGGCTTGAAGATG-3′.

Proliferation assay

Lymph node cells were prepared from BALB/c mice, labeled with CFSE (2 μM in PBS) at 37°C for 10 min, and washed with complete RPMI 1640 medium. Then, 0.5–1 $\times$ 10^5 labeled lymphocytes were cultured with isolated TAMs or spleen macrophages at a 3:1 ratio in the presence of anti-CD3 (1 μg/ml) and anti-CD28 Abs (0.5 μg/ml) in triplicates in a 96-well round-bottom plate. The proliferation of total cells was tested by CFSE dilution using flow cytometry on day 3, and the cell-proliferation rate was calculated.

Measurement of IFN-γ–secreting T cells by ELISPOT assay

Splenocytes were added at 1 $\times$ 10^6/well into a 96-well MSIPS45 plate (Millipore), which was precoated with rat anti-mouse IFN-γ (U-CyTech). 3T3/NKb or TUBO cells were added as APCs over the spleen cells, and 3T3/Kb or CT26 cells were used as control. The ratio of responder cells to APC was 10:1.

Tumor-infiltrating CD8$^+$ T cells were enriched from tumor cell suspension by double Percoll density gradients (36 and 63%). The enriched cell suspensions were incubated with PE-conjugated CD8$^+$ mAb (clone 12-

0081; eBioscience), followed by anti-PE mAb coupled to magnetic beads, and sorted using MS MACS columns and the Midi MACS system (both from Miltenyi Biotec) (>80% $CD8^+$ cells by flow cytometry). A total of 5×10^4–2×10^5 cells were added the wells of a 96-well MSIPS45 plate precoated with rat anti-mouse IFN-γ, and cocultured with APCs at 10:1 ratio in RPMI 1640 medium with the addition of 50 U/ml IL-2 (Sihuan Pharm). TUBO cells were exposed to 10 ng/ml IFN-γ for 24 h prior to plating with tumor-infiltrating lymphocytes (TILs) to increase the expression of MHC class I. After 36–48 h of incubation, cells were removed, and ELISPOTs were developed following the manufacturer's instructions (U-CyTech), counted, and quantified with a CTL-ImmunoSpot S6 Micro Analyzer (Cellular Technology). The results were expressed as the number of cytokine-producing cells.

Statistical analysis

Statistical significance was calculated by the Student *t* test, unless otherwise stated, with $p < 0.05$ considered statistically significant. Two-way ANOVA was performed to assess the differences in tumor growth between groups. Data are mean ± SEM of representative experiments, unless stated otherwise.

Results

Tumor progression is highly correlated with macrophage infiltration

Because the therapeutic effect of anti-Her2/neu Ab treatment depends on adaptive immunity (13–15), we reasoned that the immunosuppressive mechanisms within tumors might contribute to tumor resistance to anti-Her2/neu therapy. To this end, we dynamically analyzed the immune contexture inside the growing tumor of the Her2/neu-dependent cell line TUBO. In the early stage of tumor growth (<5 d after tumor inoculation), few $CD45^+$ leukocytes were seen in tumor tissues. By day 9 after tumor inoculation, tumor-infiltrating $CD45^+$ cells were obvious, and the number increased rapidly with tumor growth (Fig. 1A). More than half of the infiltrating $CD45^+$ cells were $CD11b^+$ myeloid cells, which could be divided into three populations: $Ly6c^{low}Gr\text{-}1^{high}$ G-MDSCs, $Ly6c^{high}Gr\text{-}1^{low/-}$ M-MDSCs, and a $Ly6c^-Gr\text{-}1^-$ population. The $Ly6c^-Gr\text{-}1^-$ population accounted for ∼70% of $CD11b^+$ cells, whereas G-MDSCs and M-MDSCs each accounted for ∼10% of $CD11b^+$ cells. The majority (>80%) of $Ly6c^-Gr\text{-}1^-$ $CD11b^+$, which coexpressed F4/80 and CD11c, should be TAMs (Fig. 1B), whereas G-MDSCs and M-MDSCs had no expression of F4/80 and CD11c (data not shown). The data suggest that the number of TAMs increased more dramatically with tumor growth compared with other tumor-infiltrating leukocytes.

The percentage of TAMs in tumor-infiltrating $CD45^+$ cells also increased after tumor inoculation (19.9, 28.6, and 47.8% at days 9, 12, and 15, respectively). The absolute number of TAMs increased linearly 15-fold between days 9 and 15 (Fig. 1C). However, tumor-infiltrating T and NK cells increased in the early stage of tumor growth but did not increase further after day 12 (Fig. 1D). Correspondingly, the ratio of TAM/CD8 T cell or TAM/NK cell did not change from days 9 to 12, but suddenly increased by 5-fold since day 15 after tumor inoculation (Fig. 1E). The number of tumor-infiltrating regulatory T cells did not increase as the tumor grew (data not shown). These results indicate that TAMs are a disproportionately increased subpopulation in TUBO tumor tissue and correlate highly with more established and progressive tumors.

TAMs with M2 phenotype confer immune tolerance and resistance to anti-Her2/neu therapy

To characterize the TAMs in the $Her2/neu^+$ breast tumor model, TAMs were purified by sorting, and real-time PCR was performed to detect the expression of various functional molecules. Compared with splenic macrophages ($CD11b^+F4/80^+$) from tumor-bearing or naive mice, TAMs ($CD11b^+F4/80^+$) expressed higher levels of the M2-type genes *Il10*, *Tgf-β*, and *Vegf* but lower levels of the M1-type genes *Il12* and *Tnf-α*. The expression of these genes in splenic macrophages was comparable between tumor-bearing mice and naive mice. (Fig. 2A). In addition, the sorted TAMs dramatically inhibited T cell proliferation stimulated with anti-CD3 and anti-CD28 mAbs, whereas the splenic macrophages from the same tumor-bearing mice had no suppressive effects (Fig. 2B). These results show that the macrophages were skewed toward the typical M2 phenotype in the tumor microenvironment, which manifested strong immunosuppressive effects.

To determine whether TAMs contribute to extrinsic resistance to anti-Her2/neu therapy, TUBO-bearing mice were treated i.p. with the well-characterized anti-Her2/neu (rat homolog of human Her2) mAb 7.16.4 (13), followed by continuous i.t. injection of clodronate liposomes (CELs) to delete TAMs (using vehicle liposome as control). Even for larger tumors in which anti-Her2/neu treatment followed by i.t. injection of vehicle liposome only slightly delayed their growth, TAM deletion following anti-Her2/neu treatment resulted in the regression of all tumors (Fig. 2C). The tumors continued to shrink even after the cessation of CEL injections, suggesting that tumor regression is mediated by an antitumor immune response. To assess whether removal of TAMs increased the tumor-specific $CD8^+$ T cell responses, the sorted tumor-infiltrating $CD8^+$ T cells or splenocytes were stimulated with 3T3/NKb cells expressing Her2/neu and $H\text{-}2K^d$ (3T3/Kb as negative control) (28) or TUBO tumor cells (CT26 as negative control) 8 d after completion of CEL injections, and IFN-γ–secreting cells were evaluated by ELISPOT. Both tumor-infiltrating $CD8^+$ T cells and splenocytes from the TAM-deleted group had 3-fold more IFN-γ–producing cells than did those from the vehicle liposome–treated group (Fig. 2D), indicating the increased responses of local and systemic tumor-specific T cells. Overall, our data suggest that TAMs confer an immune-suppressive environment that inhibits antitumor T cell responses and results in the emergence of further extrinsic resistance to anti-Her2/neu therapy.

Intratumoral treatment of IL-21 dramatically increases the therapeutic effect of anti-Her2/neu Ab

Next, we tried a series of combination treatments to manipulate the immune responses, including anti-CD137 agonist mAb, anti–programmed cell death protein 1 (PD-1)–blocking mAb, and rIL-15/IL-15Rα fusion protein to improve the therapeutic effect of anti-Her2/neu Ab. Impressively, i.t. injection of IL-21 resulted in the most notable therapeutic effects combined with anti-Her2/neu treatment. Injection of low-dose IL-21 (5 μg) alone had no effect on tumor growth, and anti-Her2/neu treatment alone delayed tumor growth compared with control treatment; however, the combination of these two treatments rapidly eradicated the tumor masses in all mice (Fig. 3A). Neu-transgenic mice are tolerant to Rat-neu and are highly resistant to various immunotherapies or anti-neu Ab. The same therapeutic regimen even rapidly eradicated the established TUBO tumors in all tolerant F1 neu-transgenic mice (BALB/c × FVB/N MMTV-neu) (Fig. 3B). The cured mice rejected the rechallenged tumors, suggesting that long-term immune memory was generated (Fig. 3C). However, the i.v. injection of 5-fold more IL-21 had no synergistic antitumor effect with anti-Her2/neu Ab, suggesting the local effect of IL-21 on tumors (Fig. 3D). These results demonstrate that tumor local delivery of IL-21 could overcome the extrinsic resistance of tumors to anti-Her2/neu therapy and markedly improve the antitumor effects of anti-Her2/neu Ab.

Intratumoral IL-21 directly skews TAM polarization

Although the antitumor effects of IL-21 are considered to be mediated by NK and/or $CD8^+$ T cells (31–33), their local effects on tumor tissues in the combination therapy with anti-Her2/neu Ab promoted us to pursue their effects on TAMs. Tumor-bearing

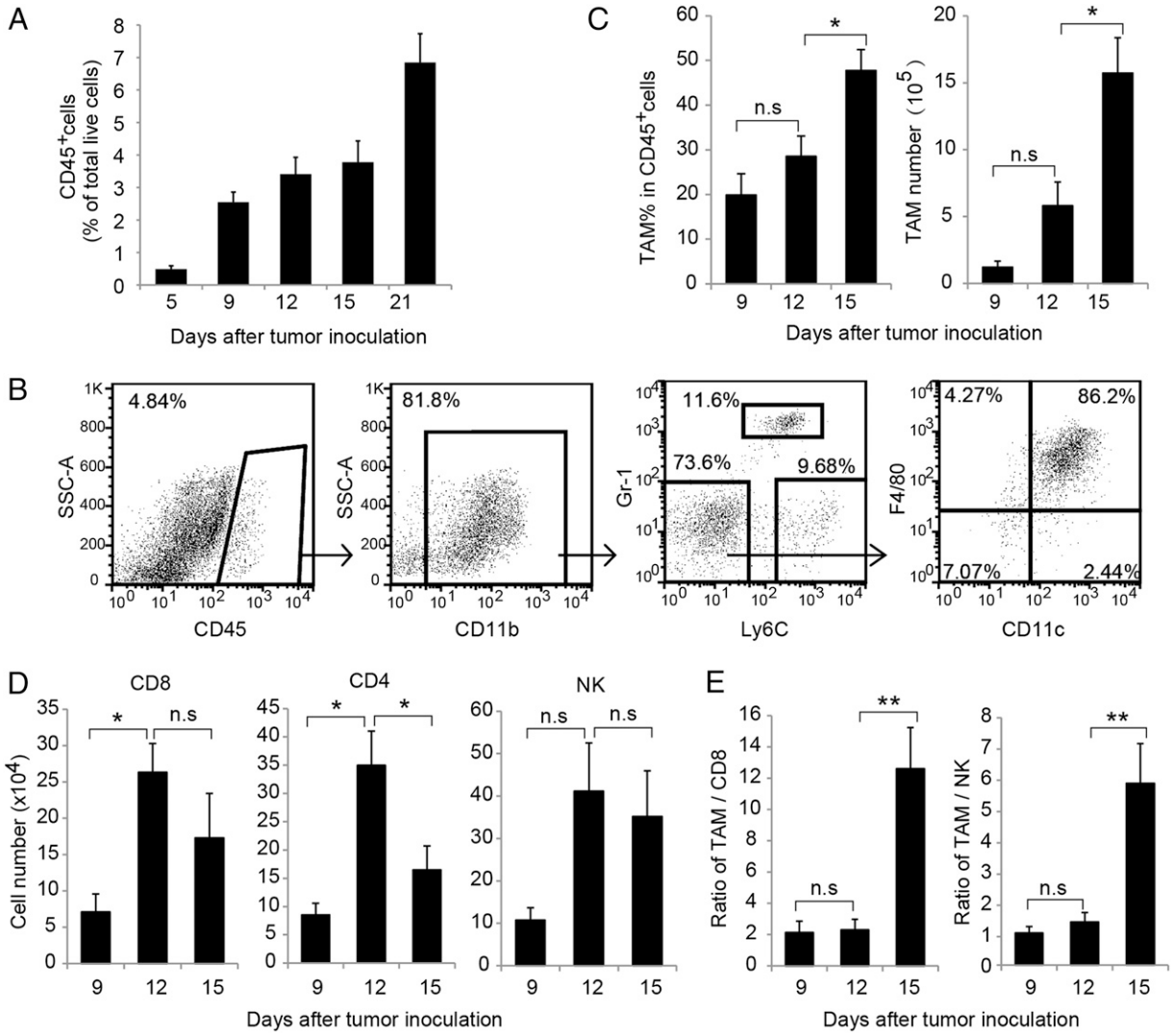

FIGURE 1. Correlation of macrophage infiltration with tumor progression. BALB/c mice (n = 3–5) were injected s.c. with 8–10 × 10^5 TUBO cells and sacrificed at the indicated time points. Tumor-infiltrating myeloid-derived cells and lymphocytes were evaluated by flow cytometry. (**A**) Percentages of tumor-infiltrating $CD45^+$ cells. (**B**) Gating strategy for analysis of TAMs ($CD45^+CD11b^+Gr1^-Ly6C^-F4/80^+CD11c^+$). (**C**) Percentage and absolute number of TAMs. (**D**) Absolute numbers of tumor-infiltrating $CD8^+$, $CD4^+$, and NK cells. (**E**) The ratio of macrophages/$CD8^+$ T cells or macrophages/NK cell in tumors. Data are mean ± SEM and are representative of five independent experiments. *$p < 0.05$, **$p < 0.01$. n.s, not significant.

mice were injected i.t. with rIL-21 or PBS on days 15 and 17 after tumor inoculation, and the expression of the M1/M2-type genes in TAMs sorted from tumor masses was detected by real-time PCR 3 d after the last injection of IL-21. TAMs from the IL-21–treated group expressed reduced levels of M2-type genes *Tgf-β*, *Il10*, *Ccl17*, *Vegf*, and *Arg2* compared with TAMs from the control group. In contrast, the M1-type genes *Cxcl9* and *iNos* tended to be upregulated in TAMs from the IL-21–treated group (Fig. 4A). Instead of inhibiting T cell proliferation, TAMs from IL-21–treated tumors enhanced T cell proliferation (Fig. 4B). Immunohistochemistry analysis showed that IL-21 treatment significantly increased the expression of CD86 on TAMs, whereas it tended to reduce the tumor infiltration of macrophages and enhance MHC class II expression on TAMs (Supplemental Fig. 1).

To test the antitumor effect of IL-21 through TAM polarization in other tumor models, we combined tumor local treatment of IL-21 with the chemotherapeutic doxorubicin in an MCA205 tumor model. Doxorubicin treatment alone had minimal effect on tumor growth, whereas combination with IL-21 treatment dramatically improved its therapeutic effect (Supplemental Fig. 2A). Similarly, i.t. injection of IL-21 significantly decreased the expression of M2-type genes *Ccl17*, *Tgf-β*, and *Vegf* in sorted TAMs from MCA205 tumors (Supplemental Fig. 2B). These results demonstrate that tumor local treatment of IL-21 skewed TAM polarization away from the immune-suppressive M2 phenotype toward the immune-stimulatory M1 phenotype.

TAM polarization induced by intratumoral delivery of IL-21 might be explained by the stimulation of tumor-infiltrating $CD8^+$ T cells and NK cells to produce IFN-γ, a strong stimulator of M1 polarization of macrophages. To exclude this possibility, tumor-bearing $Rag^{-/-}$ mice were injected i.p. with anti-asialo GM1 Ab 5 d before the first i.t. injection of IL-21. TAMs from IL-21–treated mice lacking T, B, and NK cells still upregulated the expression of the M1-type gene *iNos* and downregulated the expression of the M2-type genes *Il10*, *Ccl17*, *Vegf*, and *Tgf-β* to a greater extent than did TAMs from IL-21–treated wild-type mice (Fig. 4C, compared with Fig. 4A). These results suggest that TAM polarization skewed by IL-21 treatment is independent of T, B, or NK cells.

To assess the direct effect of IL-21 on TAM polarization, the freshly sorted TAMs were cultured with IL-21 overnight. They expressed reduced levels of the M2-type genes *Vegf* and *Tgf-β*, but increased levels of the M1-type gene *Ccl2*, compared with TAMs from the control group (Fig. 4D). In addition, the in vitro treatment of IL-21

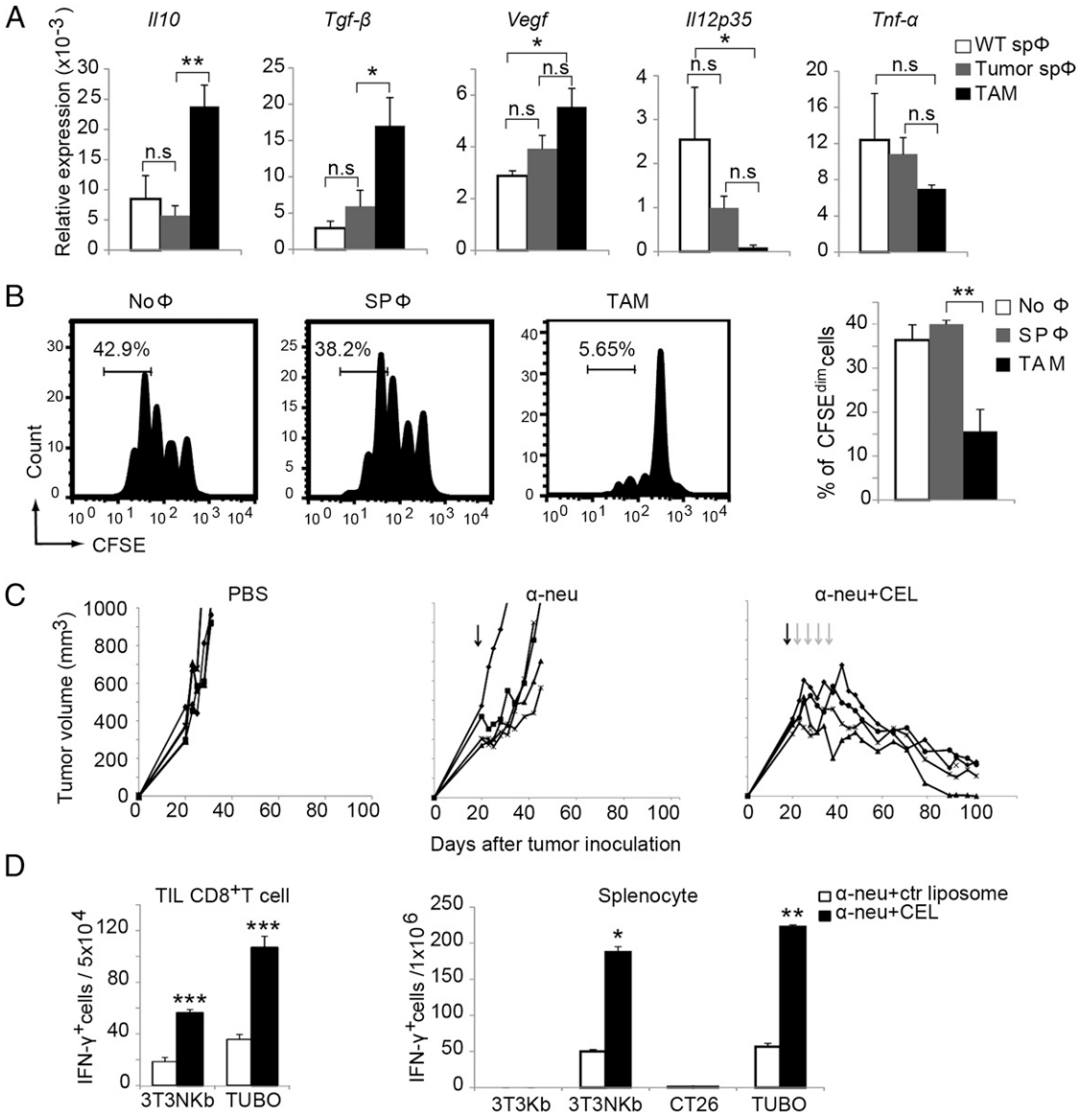

FIGURE 2. TAMs manifest the M2 phenotype and suppress the antitumor response triggered by anti-Her2/neu Ab. (**A** and **B**) BALB/c mice ($n = 3–5$) were inoculated s.c. with 1×10^6 TUBO cells and sacrificed after 15 d. (A) qPCR was performed on FACS-sorted TAMs and spleen macrophages from the same tumor-bearing mice (tumor spΦ) or naive mice (WT spΦ). Relative copy number of M2- and M1-type cytokines to *β-actin*. (B) The sorted TAMs or spleen macrophages were cocultured with CFSE-labeled naive lymph node cells at 1:3 ratio in the presence of anti-CD3 and anti-CD28 Abs. T cell proliferation was measured by CFSE dilution after 72 h. The percentages of CFSE-dim cells (at least four divisions) were calculated. (**C**) Tumor-bearing mice ($n = 5$) were treated i.p. with 200 μg anti-Her2/neu on day 19. CELs or control liposomes (6.25 μg) were administered i.t., every 4 d, from days 23 to 35, as indicated by the arrows. (**D**) Tumor-bearing mice ($n = 5$) were treated i.p. with 100 μg anti-Her2/neu on day 19. CEL or control liposomes (6.25 μg) were injected i.t. every 3 d from day 24 to 36. Mice were sacrificed on day 44. Sorted $CD8^+$ TILs (*left panel*) or total splenocytes (*right panel*) were stimulated with 3T3/NKb, 3T3/Kb, TUBO, or CT26 cells at a 10:1 ratio. IFN-γ–producing cells were enumerated by ELISPOT assay. Results are expressed as the number of spots/5×10^4 $CD8^+$ TILs or 1×10^6 splenocytes. Data are mean ± SEM and are representative of three independent experiments. $^*p < 0.05$, $^{**}p < 0.01$, $^{***}p < 0.001$. n.s, not significant.

also decreased the expression of the M2-type genes *Vegf* and *Il10* in bone marrow–derived macrophages (Supplemental Fig. 3A) and *Vegf*, *Tgf-β*, *Il10*, and *Ccl17* in peritoneal macrophages, and it markedly increased the expression of the M1-type genes *Tnf-α* and *Il6* in peritoneal macrophages induced by a low dose of LPS (Supplemental Fig. 3B); this suggested that the effect of IL-21 on macrophage polarization was not specific to TAMs. These results indicate that IL-21 could directly skew macrophages away from the M2 phenotype.

IL-21 amplifies the tumor-specific $CD8^+$ T cell response through polarizing TAMs

Our previous study showed that anti-Her2/neu Ab treatment increased tumor infiltration of $CD8^+$ T and NK cells (13). Flow cytometry and immunohistochemistry analysis showed that the combination treatment of IL-21 and anti-Her2/neu Ab further increased tumor-infiltrating $CD8^+$ T cells by 2-fold, which reached 20% of tumor-infiltrating $CD45^+$ cells, but failed to increase $CD4^+$ T cells and NK cells in tumors compared with anti-Her2/neu Ab alone (Fig. 5A, 5B). Strikingly, the percentage of IFN-γ–producing cells among tumor-infiltrating $CD8^+$ T cells from the combined treatment group was also 2-fold more than that of the anti-Her2/neu group (Fig. 5C). Thus, tumor local delivery of IL-21 increased the quantity and enhanced the function of $CD8^+$ T cells in tumors treated with anti-Her2/neu Ab.

To underscore the role of TAM polarization skewed by IL-21 treatment in our combination therapy, we compared the effects

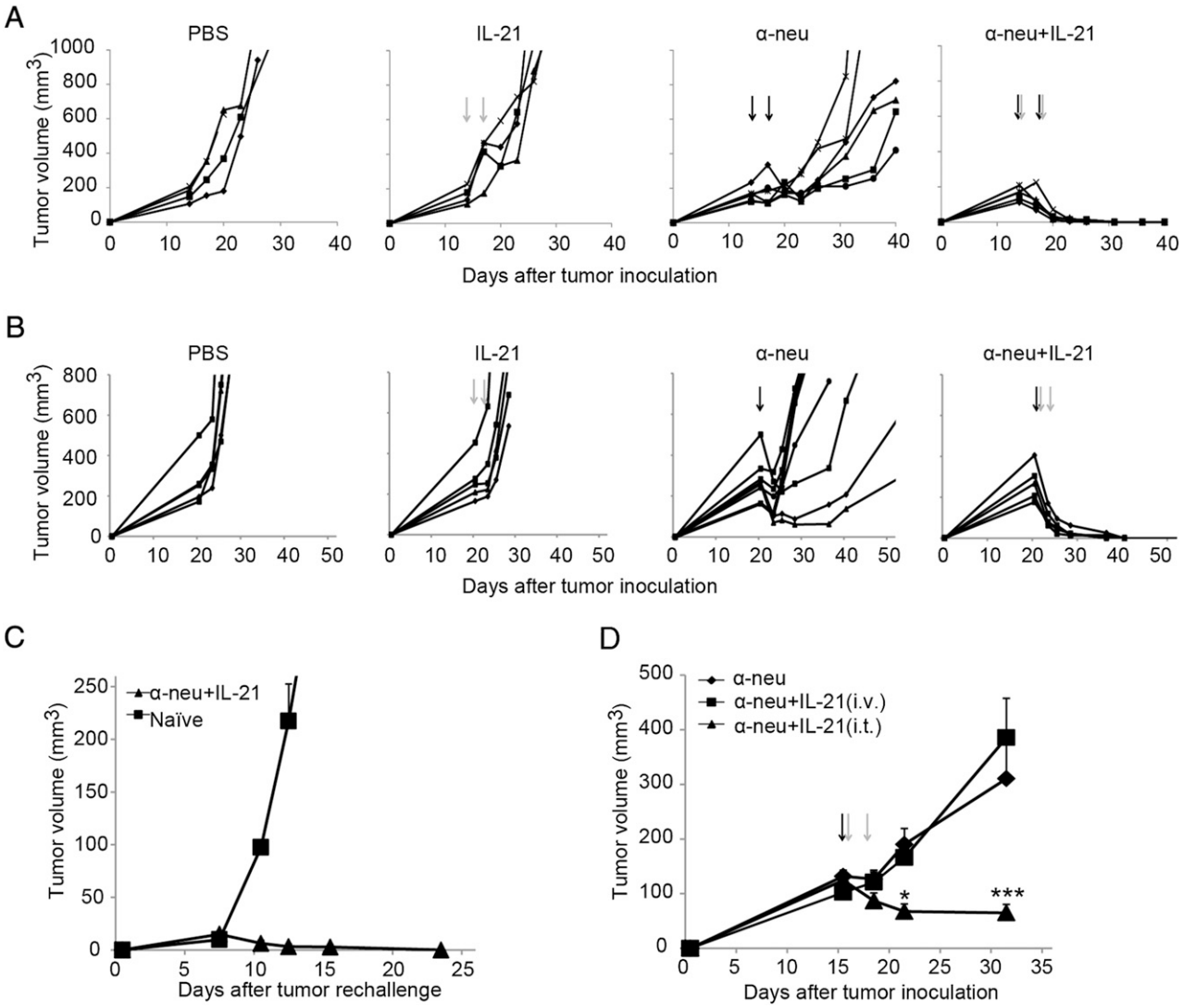

FIGURE 3. Combination therapy of anti-Her2/neu Ab with tumor local IL-21. (**A**) TUBO-bearing mice ($n = 5$) were treated i.p. with 100 μg anti-Her2/neu and/or i.t. with 5 μg IL-21 (PBS as control) on days 14 and 17, as indicated by arrows. (**B**) TUBO-bearing Neu-transgenic F1 mice ($n = 5$–7) were treated i.p. with 150 μg anti-Her2/neu on day 20 and injected i.t. with 5 μg IL-21 (PBS as control) on days 20 and 23, as indicated by the arrows. (**C**) The cured mice or naive mice ($n = 5$) were rechallenged s.c. with 5×10^6 TUBO cells on the opposite side from the primary tumors ≥1 mo after complete rejection of primary tumors. (**D**) Tumor-bearing mice ($n = 5$) were treated i.p. with 100 μg anti-Her2/neu on day 15 and injected i.v. with 25 μg or injected i.t. with 5 μg IL-21 on days 15 and 17. Data are representative of three (A and B) or two (C and D) independent experiments. $^*p < 0.05$, $^{***}p < 0.001$, i.v. versus i.t., two-way ANOVA.

of TAM deletion on therapy with anti-Her2/neu Ab alone and combination therapy. Anti-Her2/neu treatment alone only delayed the tumor growth, whereas TAM deletion following Ab treatment markedly enhanced the therapeutic effects of anti-Her2/neu Ab, which resulted in tumor regression in four of six mice, indicating that TAMs were predominantly of tumor-promoting M2 phenotype in Ab-treated tumors. Conversely, combination therapy of anti-Her2/neu and IL-21 resulted in rapid elimination of all detectable tumors, whereas the TAM deletion prevented the tumor regression induced by the combination treatment and caused rapid grow-up of tumors in two of six mice, suggesting that TAMs are tumor-inhibitory M1 phenotype in tumors with the combination treatment (Fig. 5D). Concomitant with the contrary polarization of TAMs with anti-Her2/neu Ab alone and combination therapy, TAM deletion increased IFN-γ−producing $CD8^+$ T cells in tumors treated with anti-Her2/neu Ab alone while dramatically reducing IFN-γ−producing $CD8^+$ T cells in tumors treated with combination therapy to the same level as that seen with anti-Her2/neu monotherapy (Fig. 5E). Collectively, these results show that the combination treatment of IL-21 and anti-Her2/neu Ab can greatly amplify the tumor-specific $CD8^+$ T cell response in the tumor microenvironment triggered by anti-Her2/neu therapy through reprogramming TAMs from the M2 phenotype to the M1 phenotype. Moreover, the reprogrammed M1 TAMs are required for the tumor regression mediated by the combination therapy of anti-Her2/neu and IL-21.

Discussion

In this study, we found that TAMs with the M2 phenotype are gradually enriched within growing tumors and confer tumor resistance to anti-Her2/neu therapy as a major extrinsic limitation. Next, we demonstrated an effective strategy to prevent anti-Her2/neu–resistant breast cancer: combination therapy using anti-Her2/neu Ab and tumor local IL-21. The mechanism underlying its superior effect is that IL-21 has the potential to skew TAMs away from the immune-suppressive M2 phenotype and, therefore, break the immune tolerance of the tumor microenvironment.

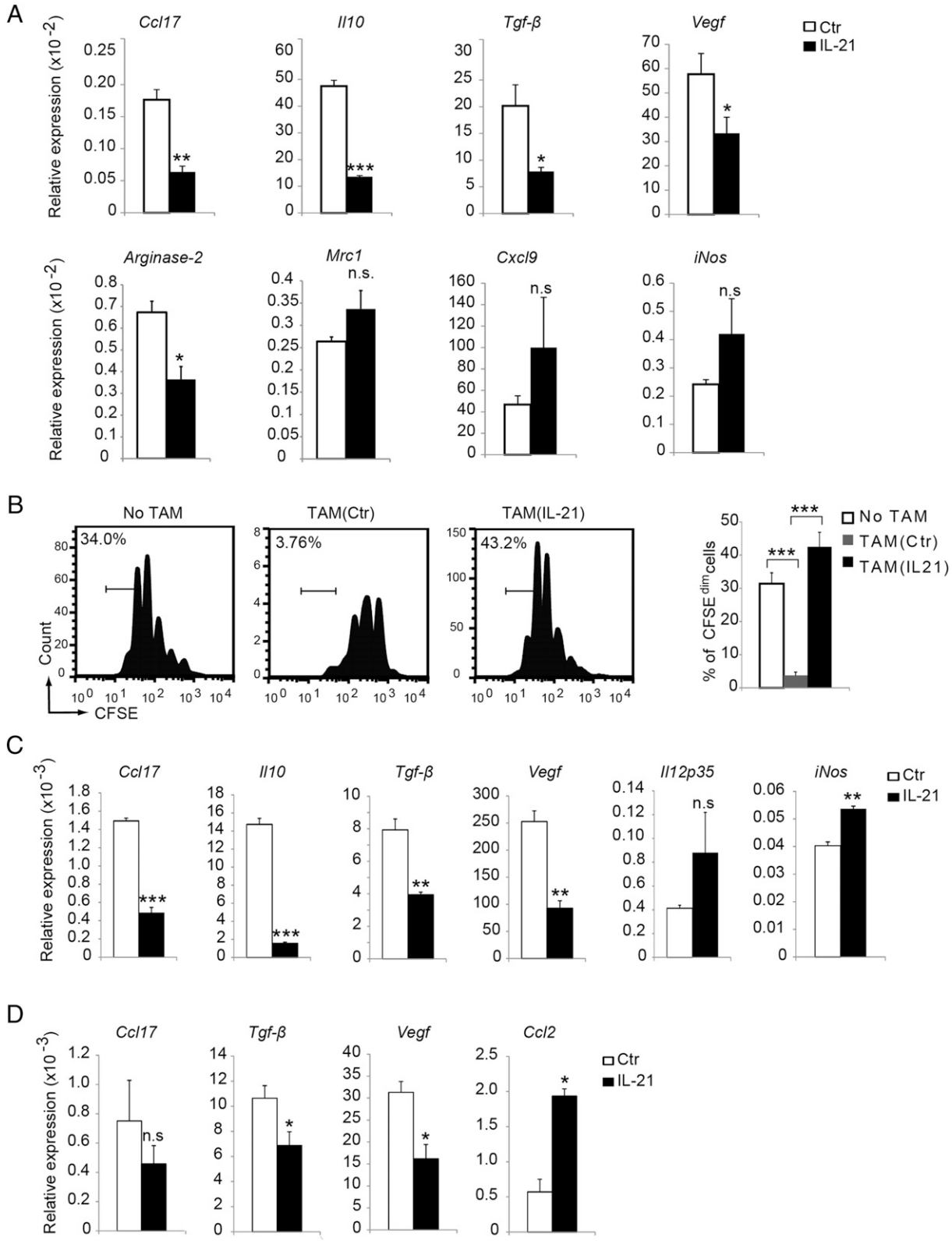

FIGURE 4. IL-21 skews TAMs away from the M2 phenotype and toward the M1 phenotype. (**A** and **B**) Tumor-bearing mice (n = 3–5) were injected i.t. with 5 μg IL-21 on days 15 and 17, and the tumor was excised on day 20. (A) qPCR was performed on sorted TAMs. Relative copy number was calculated based on *β-actin*. (B) CFSE-labeled lymph node cells were cocultured with sorted TAMs at a 3:1 ratio in the presence of anti-CD3 and anti-CD28 Abs for 3 d. T cell proliferation was measured by CFSE dilution. The percentages of $CFSE^{dim}$ cells (at least five divisions) were calculated. (**C**) TUBO-bearing Rag-$1^{-/-}$ mice (n = 3) were administered 50 μg anti-asialo GM1 Ab i.p. every 4 d, starting on day 13. IL-21 was injected i.p. on days 18, 20, and 21, and tumors were excised on day 22. qPCR was performed on sorted TAMs. Relative copy number was calculated based on *β-actin*. (**D**) TAMs were sorted from established TUBO tumors and exposed to IL-21 (100 ng/ml) for 16 h. Relative copy numbers of M2- and M1-type cytokines to *β-actin* were detected by qPCR. Data are mean ± SEM and are representative of three independent experiments. $*p < 0.05$, $**p < 0.01$, $***p < 0.001$. n.s, not significant.

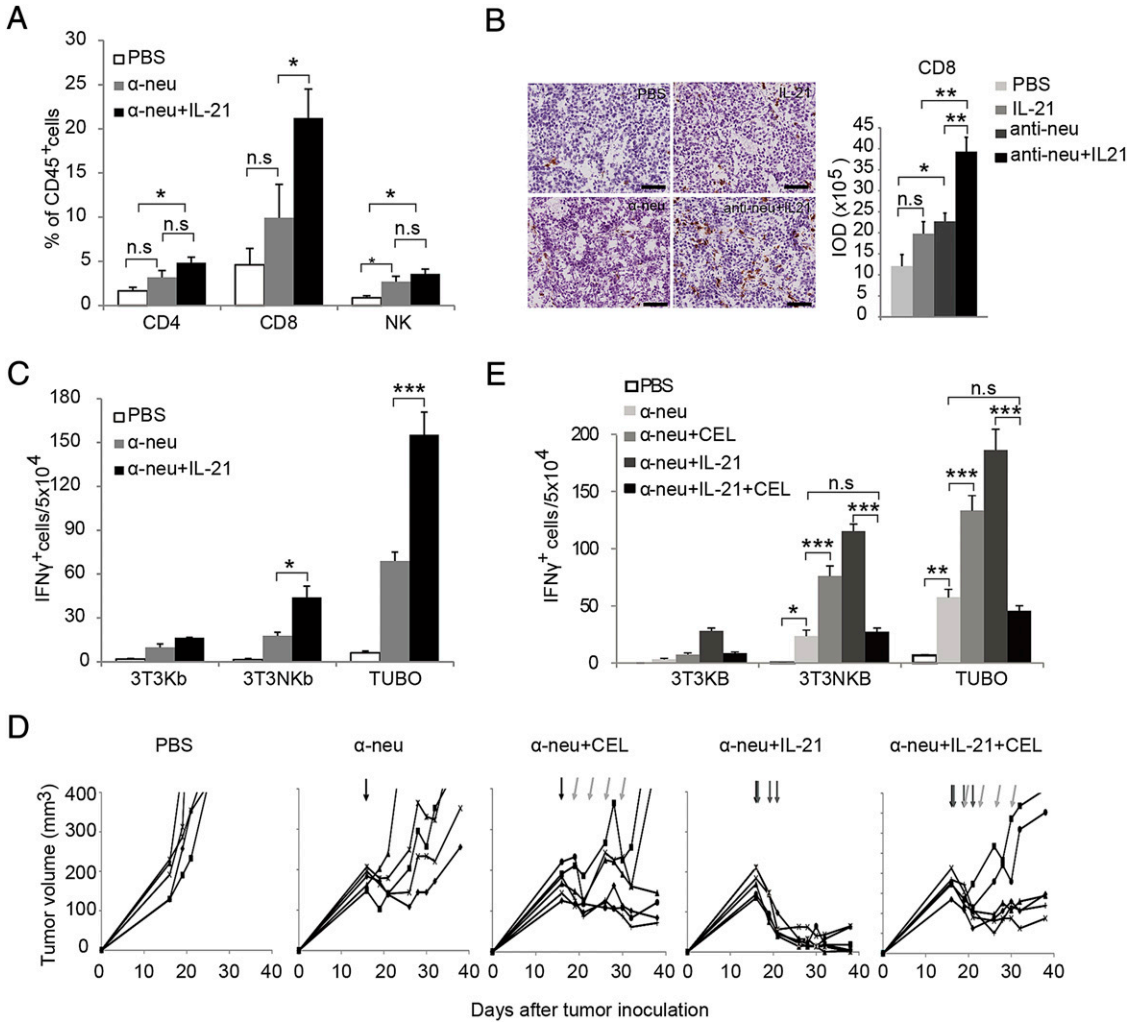

FIGURE 5. Opposite effects of TAM deletion on augmented tumor-reactive CD8$^+$ T cell response triggered by monotherapy of anti-Her2/neu and combination therapy of anti-Her2/neu and IL-21. (**A**) Tumor-bearing mice ($n = 5$) were treated i.p. with 200 μg anti-Her2/neu on day 15 and were injected i.t. with 5 μg IL-21 on days 15 and 17. Mice were sacrificed on day 20. Percentages of different TIL populations are shown. (**B**) Immunohistochemistry for CD8 was performed on frozen sections of tumors 3 d after the last treatment. Results are shown as representative photographs (*left panels*) and as integral OD of positive cells/three microscope fields for each sample ($n = 6$) (*right panel*). Scale bars, 73 μm. (**C**) Purified CD8$^+$ TILs were stimulated with 3T3/Kb, 3T3/NKb, or TUBO cells at 10:1 ratio. IFN-γ–producing cells were enumerated by ELISPOT assay after a 48-h coculture. IFN-γ$^+$ cells are expressed as the number of spots/5 $\times$ 10^4 CD8$^+$ TILs. (**D**) Tumor-bearing mice ($n = 5$) were treated i.p. with 200 μg anti-Her2/neu on day 16 and were injected i.t. with 5 μg IL-21 on days 16, 19, and 21. CELs or control liposomes were administered i.p. (12.5 μg) every 4 d from days 19 to 31, as indicated by the arrows. (**E**) Tumor-bearing mice ($n = 5$) were treated i.p. with 200 μg anti-Her2/neu on day 18 and were injected i.t. with 5 μg IL-21 on days 18 and 20. CELs or control liposomes were administered i.p. (12.5 μg) on days 20 and 24. Tumors were excised on day 28, and IFN-γ–producing CD8$^+$ TILs were detected by ELISPOT assay. Results are expressed as the number of spots/5 $\times$ 10^4 CD8$^+$ TILs. Data are mean $\pm$ SEM and are representative of three (A, B, D, and E) or five (C) independent experiments. $^*p < 0.05$, $^{**}p < 0.01$, $^{***}p < 0.001$. n.s, not significant.

Recent work showed convincingly that Ab-mediated tumor control depends on both innate and adaptive immune responses (13–15). However, multiple immune-suppressive mechanisms in the cancer microenvironment impair antitumor immunity and promote tumor recurrence. Targeting intrinsic signaling of tumor cells, as well as the extrinsic immune-suppressive microenvironment, will enhance the ongoing immune response against tumor, resulting in sustained tumor remission (34, 35). One of the most successful strategies is blockade of the B7-H1(PD-L1)/PD-1 pathway. Recent clinical trials demonstrated that ~40% of patients treated with human anti-PD1 Ab had objective responses, with a durable response observed in only 20% of patients (36). Although this is an exciting strategy because this treatment has a much higher success rate than conventional treatment, the majority of patients still fail to respond to anti-PD1 treatment. Other strategies need to be considered.

The tumor microenvironment contains various cellular and molecular immune-suppressive mechanisms. Different tumors might rely on different key dominant immune-resistant mechanisms. In this TUBO breast cancer model, PD-1 is highly expressed on tumor-infiltrating CD8$^+$ T cells. Blockade of PD-1 signaling by anti–PD-1 Ab improves the therapeutic activity of anti-Her2/neu therapy (15). However, this therapeutic strategy is not the most optimal combinatorial treatment with regard to anti-Her2/neu Ab, especially for larger or advanced tumors (data not shown); this suggests that, in addition to the PD-1 signaling pathway, other immune-suppressive mechanisms are responsible for resistance to anti-Her2/neu therapy. In this study, we characterized the abundant M2 TAMs in HER2/neu$^+$ breast tumor as a dominant extrinsic limitation to confer tumor resistance to anti-Her2/neu Ab therapy. This is consistent with a recent clinical study demonstrating that stromal infiltration of CD68$^+$ macrophages correlated

inversely with the presence of $CD8^+$ T cells in human breast cancer tissues and that the CD68/CD8 immune signature is an independent prognostic indicator for survival (20, 37). Thus, a similar phenotype of TAMs might exist and mediate resistance to anticancer therapy in human breast cancer. TAMs are recognized as a promising target for tumor therapy, and reduction of their tumor-promoting activities has become a hot topic. TAM-targeted antitumor approaches principally include inhibition of macrophage recruitment and survival in tumor and blockade of the tumor-promoting activity of TAMs. Macrophages are highly plastic and can adopt a different phenotype depending on the changing milieu. TAMs can be re-educated to become tumoricidal or tumor-suppressive M1-like phenotype. Nonetheless, only a few molecules have been identified to orchestrate this process (25, 38, 39).

IL-21, a pleiotropic common γ-chain (γc) cytokine, is primarily produced by activated $CD4^+$ T cells and NKT cells, but it acts on multiple lineages, including T cells, B cells, NK cells, NKT cells, and dendritic cells. It should be noted that the role of IL-21 is well established in T and B cells, but it is less well studied in innate immunity (40, 41). Although several studies demonstrated the complex effects of IL-21 on dendritic cells (42, 43), its role in other myeloid cells is poorly documented. It was reported that monocytes/macrophages express IL-21R, and stimulation of IL-21 in vitro enhances phagocytosis and protease activity of monocytes/macrophages (44–47). Our present study reveals an unprecedented role for IL-21 in re-educating TAMs. We found that tumor local delivery of IL-21 can shift TAM polarization from the immune-suppressive M2 phenotype to the tumor-inhibiting M1 phenotype, which dramatically promotes anti-Her2/neu Ab therapy. The polarization is a direct action of IL-21 on TAMs, but it is not mediated by IFN-γ produced by IL-21–activated $CD8^+$ T cells and/or NK cells, because in vitro stimulation of IL-21 can rapidly skew the polarization of sorted TAMs; elimination of T, B, and NK cells enhances, instead of diminishes, the tumor local IL-21–induced polarization of TAMs to the M1 phenotype; and depletion of TAMs decreases the progression of anti-Her2/neu–treated tumors while increasing the growth of tumors treated with anti-Her2/neu and IL-21, implying that TAMs acquired a tumor-suppressive M1-like phenotype when exposed to local IL-21. Treatment with IL-21 alone also decreased the expression of the M2-type genes *Vegf* and *Il10* in M-CSF–induced bone marrow–derived macrophages and *Vegf*, *Tgf-β*, *Il10*, and *Ccl17* in peritoneal macrophages. These results were contrary to the study by Pesce et al. (48), in which pretreatment of bone marrow–derived macrophages with IL-21 increased the expression of the M2-type genes *Arg-1* and *FIZZ1* when subsequently stimulated with IL-4 and IL-13. This difference may suggest that macrophage programing by IL-21 depends on the environment of the macrophages. Thus, more research is required to define the effects of IL-21 on macrophages in various conditions.

IL-21 had significant antitumor activity against a variety of tumors in preclinical studies, and it is in a phase II clinical trial for metastatic melanoma (49–52). Depending on the tumor type and the methods of IL-21 application, the antitumor effect of IL-21 was mediated by $CD8^+$ T cells, NK cells, or both. Most of these studies were done by deleting $CD8^+$ T cells or NK cells with Abs. However, it is well known that antitumor $CD8^+$ T cells or/and NK cells in the tumor microenvironment are firmly harnessed by a plethora of immune-suppressive mechanisms, so that they cannot be fully activated if the immune-suppressive mechanisms are not blocked or ameliorated. Therefore, our studies suggest that, in well-established tumors, such as larger or advanced tumors, skewing TAM polarization to the M1-like phenotype is the prerequisite for IL-21 to augment $CD8^+$ T cell and/or NK cell cytotoxicity to exert its antitumor effects. Otherwise, IL-21 should not be able to directly activate $CD8^+$ T cells and NK cells to eliminate the tumors because of the immune-suppressive mechanisms dominated by TAMs. IL-21–induced polarization of TAMs eliminates the immune suppression of TAMs to unleash the tumor-specific $CD8^+$ T cell response, as well as reverses the immune suppression of TAMs to simulate antitumor immune responses. Based on our data, the potential clinical applicability of IL-2–mediated programming of macrophages allows for a more broad and attractive candidate for combination with Ab, as well as with immunogenic chemotherapy, irradiation, and novel immunotherapeutic agents, such as adoptive transfer of TCR-engineered T cells or treatment with anti-PD1 or anti-CTLA4. Because TAM abundance, distribution, and phenotypes varied between mouse models and human patients, even within different types of human cancers, future work should aim to define the response of TAMs to IL-21 stimulation in different types and subtypes of human cancers. To overcome the shortcoming of local injection of IL-21, fusion of IL-21 with the anti-Her2/neu Ab will be a strategy for tumor-targeting the delivery of IL-21 while maintaining the antitumor effects of the Ab.

In conclusion, our study demonstrates that the M2-type of TAM plays a dominant role in extrinsic resistance to Ab therapy, which is a promising anticancer strategy. We combined Ab therapy with targeted delivery of IL-21 to efficiently break the tumor resistance when the M2 type of TAMs become dominant. Our findings unveil a role for IL-21 in reprogramming M2 TAMs and highlight the potential of using re-educated TAMs to restore the antitumor T cell response. The study provides an opportunity to develop next-generation biologics by combining anti-Her2/neu Ab with IL-21.

Disclosures

The authors have no financial conflicts of interest.

References

1. Romond, E. H., E. A. Perez, J. Bryant, V. J. Suman, C. E. Geyer, Jr., N. E. Davidson, E. Tan-Chiu, S. Martino, S. Paik, P. A. Kaufman, et al. 2005. Trastuzumab plus adjuvant chemotherapy for operable HER2-positive breast cancer. *N. Engl. J. Med.* 353: 1673–1684.
2. Hudis, C. A. 2007. Trastuzumab—mechanism of action and use in clinical practice. *N. Engl. J. Med.* 357: 39–51.
3. Piccart-Gebhart, M. J., M. Procter, B. Leyland-Jones, A. Goldhirsch, M. Untch, I. Smith, L. Gianni, J. Baselga, R. Bell, C. Jackisch, et al; Herceptin Adjuvant (HERA) Trial Study Team. 2005. Trastuzumab after adjuvant chemotherapy in HER2-positive breast cancer. *N. Engl. J. Med.* 353: 1659–1672.
4. Vogel, C. L., M. A. Cobleigh, D. Tripathy, J. C. Gutheil, L. N. Harris, L. Fehrenbacher, D. J. Slamon, M. Murphy, W. F. Novotny, M. Burchmore, et al. 2002. Efficacy and safety of trastuzumab as a single agent in first-line treatment of HER2-overexpressing metastatic breast cancer. *J. Clin. Oncol.* 20: 719–726.
5. Cobleigh, M. A., C. L. Vogel, D. Tripathy, N. J. Robert, S. Scholl, L. Fehrenbacher, J. M. Wolter, V. Paton, S. Shak, G. Lieberman, and D. J. Slamon. 1999. Multinational study of the efficacy and safety of humanized anti-HER2 monoclonal antibody in women who have HER2-overexpressing metastatic breast cancer that has progressed after chemotherapy for metastatic disease. *J. Clin. Oncol.* 17: 2639–2648.
6. Seidman, A. D., M. N. Fornier, F. J. Esteva, L. Tan, S. Kaptain, A. Bach, K. S. Panageas, C. Arroyo, V. Valero, V. Currie, et al. 2001. Weekly trastuzumab and paclitaxel therapy for metastatic breast cancer with analysis of efficacy by HER2 immunophenotype and gene amplification. *J. Clin. Oncol.* 19: 2587–2595.
7. Nagata, Y., K. H. Lan, X. Zhou, M. Tan, F. J. Esteva, A. A. Sahin, K. S. Klos, P. Li, B. P. Monia, N. T. Nguyen, et al. 2004. PTEN activation contributes to tumor inhibition by trastuzumab, and loss of PTEN predicts trastuzumab resistance in patients. *Cancer Cell* 6: 117–127.
8. Saez, R., M. A. Molina, E. E. Ramsey, F. Rojo, E. J. Keenan, J. Albanell, A. Lluch, J. Garcia-Conde, J. Baselga, and G. M. Clinton. 2006. p95HER-2 predicts worse outcome in patients with HER-2-positive breast cancer. *Clin. Cancer Res.* 12: 424–431.
9. Scaltriti, M., F. Rojo, A. Ocaña, J. Anido, M. Guzman, J. Cortes, S. Di Cosimo, X. Matias-Guiu, S. Ramon y Cajal, J. Arribas, and J. Baselga. 2007. Expression of p95HER2, a truncated form of the HER2 receptor, and response to anti-HER2 therapies in breast cancer. *J. Natl. Cancer Inst.* 99: 628–638.
10. Nahta, R., L. X. Yuan, B. Zhang, R. Kobayashi, and F. J. Esteva. 2005. Insulin-like growth factor-I receptor/human epidermal growth factor receptor 2 heterodimerization contributes to trastuzumab resistance of breast cancer cells. *Cancer Res.* 65: 11118–11128.

11. Zhuang, G., D. M. Brantley-Sieders, D. Vaught, J. Yu, L. Xie, S. Wells, D. Jackson, R. Muraoka-Cook, C. Arteaga, and J. Chen. 2010. Elevation of receptor tyrosine kinase EphA2 mediates resistance to trastuzumab therapy. *Cancer Res.* 70: 299–308.
12. Clynes, R. A., T. L. Towers, L. G. Presta, and J. V. Ravetch. 2000. Inhibitory Fc receptors modulate in vivo cytotoxicity against tumor targets. *Nat. Med.* 6: 443–446.
13. Park, S., Z. Jiang, E. D. Mortenson, L. Deng, O. Radkevich-Brown, X. Yang, H. Sattar, Y. Wang, N. K. Brown, M. Greene, et al. 2010. The therapeutic effect of anti-HER2/neu antibody depends on both innate and adaptive immunity. *Cancer Cell* 18: 160–170.
14. Mortenson, E. D., S. Park, Z. Jiang, S. Wang, and Y. X. Fu. 2013. Effective anti-neu-initiated antitumor responses require the complex role of CD4+ T cells. *Clin. Cancer Res.* 19: 1476–1486.
15. Stagg, J., S. Loi, U. Divisekera, S. F. Ngiow, H. Duret, H. Yagita, M. W. Teng, and M. J. Smyth. 2011. Anti-ErbB-2 mAb therapy requires type I and II interferons and synergizes with anti-PD-1 or anti-CD137 mAb therapy. *Proc. Natl. Acad. Sci. USA* 108: 7142–7147.
16. Denkert, C., S. Loibl, A. Noske, M. Roller, B. M. Müller, M. Komor, J. Budczies, S. Darb-Esfahani, R. Kronenwett, C. Hanusch, et al. 2010. Tumor-associated lymphocytes as an independent predictor of response to neoadjuvant chemotherapy in breast cancer. *J. Clin. Oncol.* 28: 105–113.
17. Farmer, P., H. Bonnefoi, P. Anderle, D. Cameron, P. Wirapati, V. Becette, S. André, M. Piccart, M. Campone, E. Brain, et al. 2009. A stroma-related gene signature predicts resistance to neoadjuvant chemotherapy in breast cancer. *Nat. Med.* 15: 68–74.
18. Qian, B. Z., and J. W. Pollard. 2010. Macrophage diversity enhances tumor progression and metastasis. *Cell* 141: 39–51.
19. Coffelt, S. B., A. O. Tal, A. Scholz, M. De Palma, S. Patel, C. Urbich, S. K. Biswas, C. Murdoch, K. H. Plate, Y. Reiss, and C. E. Lewis. 2010. Angiopoietin-2 regulates gene expression in TIE2-expressing monocytes and augments their inherent proangiogenic functions. *Cancer Res.* 70: 5270–5280.
20. DeNardo, D. G., D. J. Brennan, E. Rexhepaj, B. Ruffell, S. L. Shiao, S. F. Madden, W. M. Gallagher, N. Wadhwani, S. D. Keil, S. A. Junaid, et al. 2011. Leukocyte complexity predicts breast cancer survival and functionally regulates response to chemotherapy. *Cancer Discov.* 1: 54–67.
21. Biswas, S. K., and A. Mantovani. 2010. Macrophage plasticity and interaction with lymphocyte subsets: cancer as a paradigm. *Nat. Immunol.* 11: 889–896.
22. Hagemann, T., T. Lawrence, I. McNeish, K. A. Charles, H. Kulbe, R. G. Thompson, S. C. Robinson, and F. R. Balkwill. 2008. "Re-educating" tumor-associated macrophages by targeting NF-kappaB. *J. Exp. Med.* 205: 1261–1268.
23. Stein, M., S. Keshav, N. Harris, and S. Gordon. 1992. Interleukin 4 potently enhances murine macrophage mannose receptor activity: a marker of alternative immunologic macrophage activation. *J. Exp. Med.* 176: 287–292.
24. Sica, A., T. Schioppa, A. Mantovani, and P. Allavena. 2006. Tumour-associated macrophages are a distinct M2 polarised population promoting tumour progression: potential targets of anti-cancer therapy. *Eur. J. Cancer* 42: 717–727.
25. Rolny, C., M. Mazzone, S. Tugues, D. Laoui, I. Johansson, C. Coulon, M. L. Squadrito, I. Segura, X. Li, E. Knevels, et al. 2011. HRG inhibits tumor growth and metastasis by inducing macrophage polarization and vessel normalization through downregulation of PlGF. *Cancer Cell* 19: 31–44.
26. Guiducci, C., A. P. Vicari, S. Sangaletti, G. Trinchieri, and M. P. Colombo. 2005. Redirecting in vivo elicited tumor infiltrating macrophages and dendritic cells towards tumor rejection. *Cancer Res.* 65: 3437–3446.
27. Rovero, S., A. Amici, E. Di Carlo, R. Bei, P. Nanni, E. Quaglino, P. Porcedda, K. Boggio, A. Smorlesi, P. L. Lollini, et al. 2000. DNA vaccination against rat her-2/Neu p185 more effectively inhibits carcinogenesis than transplantable carcinomas in transgenic BALB/c mice. *J. Immunol.* 165: 5133–5142.
28. Wei, W. Z., J. B. Jacob, J. F. Zielinski, J. C. Flynn, K. D. Shim, G. Alsharabi, A. A. Giraldo, and Y. C. Kong. 2005. Concurrent induction of antitumor immunity and autoimmune thyroiditis in CD4+ CD25+ regulatory T cell-depleted mice. *Cancer Res.* 65: 8471–8478.
29. Zhang, H., Q. Wang, K. T. Montone, J. E. Peavey, J. A. Drebin, M. I. Greene, and R. Murali. 1999. Shared antigenic epitopes and pathobiological functions of anti-p185(her2/neu) monoclonal antibodies. *Exp. Mol. Pathol.* 67: 15–25.
30. Van Rooijen, N., and A. Sanders. 1994. Liposome mediated depletion of macrophages: mechanism of action, preparation of liposomes and applications. *J. Immunol. Methods* 174: 83–93.
31. Ugai, S., O. Shimozato, K. Kawamura, Y. Q. Wang, T. Yamaguchi, H. Saisho, S. Sakiyama, and M. Tagawa. 2003. Expression of the interleukin-21 gene in murine colon carcinoma cells generates systemic immunity in the inoculated hosts. *Cancer Gene Ther.* 10: 187–192.
32. Ugai, S., O. Shimozato, L. Yu, Y. Q. Wang, K. Kawamura, H. Yamamoto, T. Yamaguchi, H. Saisho, S. Sakiyama, and M. Tagawa. 2003. Transduction of the IL-21 and IL-23 genes in human pancreatic carcinoma cells produces natural killer cell-dependent and -independent antitumor effects. *Cancer Gene Ther.* 10: 771–778.
33. Wang, G., M. Tschoi, R. Spolski, Y. Lou, K. Ozaki, C. Feng, G. Kim, W. J. Leonard, and P. Hwu. 2003. In vivo antitumor activity of interleukin 21 mediated by natural killer cells. *Cancer Res.* 63: 9016–9022.
34. Willimsky, G., M. Czéh, C. Loddenkemper, J. Gellermann, K. Schmidt, P. Wust, H. Stein, and T. Blankenstein. 2008. Immunogenicity of premalignant lesions is the primary cause of general cytotoxic T lymphocyte unresponsiveness. *J. Exp. Med.* 205: 1687–1700.
35. Gabrilovich, D. I., S. Ostrand-Rosenberg, and V. Bronte. 2012. Coordinated regulation of myeloid cells by tumours. *Nat. Rev. Immunol.* 12: 253–268.
36. Brahmer, J. R., S. S. Tykodi, L. Q. Chow, W. J. Hwu, S. L. Topalian, P. Hwu, C. G. Drake, L. H. Camacho, J. Kauh, K. Odunsi, et al. 2012. Safety and activity of anti-PD-L1 antibody in patients with advanced cancer. *N. Engl. J. Med.* 366: 2455–2465.
37. De Palma, M., and C. E. Lewis. 2011. Cancer: Macrophages limit chemotherapy. *Nature* 472: 303–304.
38. Kerkar, S. P., R. S. Goldszmid, P. Muranski, D. Chinnasamy, Z. Yu, R. N. Reger, A. J. Leonardi, R. A. Morgan, E. Wang, F. M. Marincola, et al. 2011. IL-12 triggers a programmatic change in dysfunctional myeloid-derived cells within mouse tumors. *J. Clin. Invest.* 121: 4746–4757.
39. Beatty, G. L., E. G. Chiorean, M. P. Fishman, B. Saboury, U. R. Teitelbaum, W. Sun, R. D. Huhn, W. Song, D. Li, L. L. Sharp, et al. 2011. CD40 agonists alter tumor stroma and show efficacy against pancreatic carcinoma in mice and humans. *Science* 331: 1612–1616.
40. Elsaesser, H., K. Sauer, and D. G. Brooks. 2009. IL-21 is required to control chronic viral infection. *Science* 324: 1569–1572.
41. Johnson, L. D., and S. C. Jameson. 2009. Immunology. A chronic need for IL-21. *Science* 324: 1525–1526.
42. Wan, C. K., J. Oh, P. Li, E. E. West, E. A. Wong, A. B. Andraski, R. Spolski, Z. X. Yu, J. He, B. L. Kelsall, and W. J. Leonard. 2013. The cytokines IL-21 and GM-CSF have opposing regulatory roles in the apoptosis of conventional dendritic cells. *Immunity* 38: 514–527.
43. Brandt, K., S. Bulfone-Paus, D. C. Foster, and R. Rückert. 2003. Interleukin-21 inhibits dendritic cell activation and maturation. *Blood* 102: 4090–4098.
44. Spolski, R., and W. J. Leonard. 2008. Interleukin-21: basic biology and implications for cancer and autoimmunity. *Annu. Rev. Immunol.* 26: 57–79.
45. Pelletier, M., A. Bouchard, and D. Girard. 2004. In vivo and in vitro roles of IL-21 in inflammation. *J. Immunol.* 173: 7521–7530.
46. Vallières, F., and D. Girard. 2013. IL-21 enhances phagocytosis in mononuclear phagocyte cells: identification of spleen tyrosine kinase as a novel molecular target of IL-21. *J. Immunol.* 190: 2904–2912.
47. Rückert, R., S. Bulfone-Paus, and K. Brandt. 2008. Interleukin-21 stimulates antigen uptake, protease activity, survival and induction of CD4+ T cell proliferation by murine macrophages. *Clin. Exp. Immunol.* 151: 487–495.
48. Pesce, J., M. Kaviratne, T. R. Ramalingam, R. W. Thompson, J. F. Urban, Jr., A. W. Cheever, D. A. Young, M. Collins, M. J. Grusby, and T. A. Wynn. 2006. The IL-21 receptor augments Th2 effector function and alternative macrophage activation. *J. Clin. Invest.* 116: 2044–2055.
49. Thompson, J. A., B. D. Curti, B. G. Redman, S. Bhatia, J. S. Weber, S. S. Agarwala, E. L. Sievers, S. D. Hughes, T. A. DeVries, and D. F. Hausman. 2008. Phase I study of recombinant interleukin-21 in patients with metastatic melanoma and renal cell carcinoma. *J. Clin. Oncol.* 26: 2034–2039.
50. Davis, I. D., B. Brady, R. F. Kefford, M. Millward, J. Cebon, B. K. Skrumsager, U. Mouritzen, L. T. Hansen, K. Skak, D. Lundsgaard, et al. 2009. Clinical and biological efficacy of recombinant human interleukin-21 in patients with stage IV malignant melanoma without prior treatment: a phase IIa trial. *Clin. Cancer Res.* 15: 2123–2129.
51. Davis, I. D., B. K. Skrumsager, J. Cebon, T. Nicholaou, J. W. Barlow, N. P. Moller, K. Skak, D. Lundsgaard, K. S. Frederiksen, P. Thygesen, and G. A. McArthur. 2007. An open-label, two-arm, phase I trial of recombinant human interleukin-21 in patients with metastatic melanoma. *Clin. Cancer Res.* 13: 3630–3636.
52. Petrella, T. M., R. Tozer, K. Belanger, K. J. Savage, R. Wong, M. Smylie, S. Kamel-Reid, V. Tron, B. E. Chen, N. N. Hunder, et al. 2012. Interleukin-21 has activity in patients with metastatic melanoma: a phase II study. *J. Clin. Oncol.* 30: 3396–3401.